mension that is about the same as the tip-to-surface distance. The strong lateral gradient in the electric field tends to pull the atoms to the area under the tip (*2*). This is the origin of the force between the STM tip and the Sb atoms.

As a further test of the above explanation, let us estimate the energies involved. By assuming a typical polarizability of the order of $10\ \text{Å}^3$ for the Sb atoms (*16*) and a strength for the electric field of 0.5 V/Å, we obtain an energy decrease of the order of ~0.1 eV due to the STM tip. This value is of the same order of magnitude as typical energy barriers for atomic motion on a solid surface, in support of the above explanation based on the field polarization effect (*17*).

The reversible rotation of the Sb dimers by the STM tip exhibits the features of a memory cell, in which the two orientations of each dimer represent "0" and "1," respectively. With improved control and stability of the STM tip position, it may be possible to move the Sb dimers to form, for instance, a linear chain of "bits" and to "switch" any of them by voltage pulses. The value stored in these nonvolatile memory cells can be read out by the same STM tip. Because the speed of read-write access is determined by the slow scanning speed of the STM, this type of memory device may be limited to archival memory. The density of this memory device is significantly higher than that of the current devices, because the size of each bit is only several angstroms.

Compared to other possible ways of making atomic-scale memories, dimer rotation offers an advantage in terms of reliability because the rotation process is gentle and the chance for damaging either the tip or the surface is low. The fact that the dimer orientations are stable at room temperature provides a practical advantage in operation.

REFERENCES AND NOTES

1. D. M. Eigler and E. K. Schweizer, *Nature* **344**, 524 (1990).
2. L. J. Whitman, J. A. Stroscio, R. A. Dragoset, R. J. Celotta, *Science* **251**, 1206 (1991).
3. R. S. Becker, J. A. Golovchenko, B. S. Swartzentruber, *Nature* **325**, 419 (1987).
4. I.-W. Lyo and P. Avouris, *Science* **253**, 173 (1991).
5. D. M. Eigler, C. P. Lutz, W. E. Rudge, *Nature* **352**, 600 (1991).
6. I.-W. Lyo and P. Avouris, *J. Chem. Phys.* **93**, 4479 (1990).
7. R. S. Becker, G. S. Higashi, Y. J. Chabal, A. J. Becker, *Phys. Rev. Lett.* **65**, 1917 (1990).
8. G. Dujardin, R. E. Walkup, P. Avouris, *Science* **255**, 1232 (1992).
9. Y. W. Mo, *Phys. Rev. Lett.* **69**, 3643 (1992).
10. The Si(001) surface was cleaned by thermal annealing and then allowed to cool to room temperature for deposition. The Sb_4 flux was generated by thermal evaporation from bulk Sb. After deposition, the sample was placed on the STM inside the same ultrahigh vacuum chamber for investigation.
11. D. Haneman, *Rep. Prog. Phys.* **50**, 1045 (1987), and references therein.
12. Dumbbells and rotated dumbbells are of similar stability, and they are parallel channels in the reaction path. There is no transition between these two types of clusters.
13. J. Nogami, A. A. Baski, C. F. Quate, *Phys. Rev. B* **44**, 1415 (1991); J. E. Northrup, *Phys. Rev. Lett.* **57**, 154 (1986); private communication.
14. J. D. Jackson, *Classical Electrodynamics* (Wiley, New York, 1962).
15. T. T. Tsong, *Atom-Probe Field Ion Microscopy* (Cambridge Univ. Press, Cambridge, 1990), p. 270.
16. *Handbook of Chemistry and Physics*, D. R. Lide, Ed. (CRC Press, Boca Raton, FL, ed. 73, 1992), pp. 10–198.
17. To convert the other three types of precursors (A, C, and D), the tip first needs to break them into dimers by exerting unequal forces on the four atoms in each cluster and then must rotate type B dimers into the final state.
18. I thank R. Walkup, J. Demuth, P. Avouris, D. Newns, and T. Jung for valuable discussion and assistance.

5 March 1993; accepted 13 May 1993

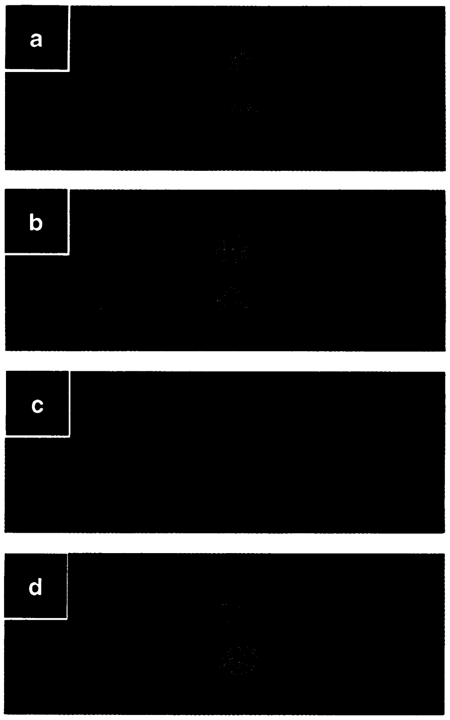

Fig. 5. The STM tip–induced displacements of two rotated dimers (in the sequence **a** through **d**). The two rotated dimers on the right move toward each other step by step until they become nearest neighbors. The two final state dimers on the left do not move.

Multiple Ion Association in Supercritical Aqueous Solutions of Single Electrolytes

Eric H. Oelkers* and Harold C. Helgeson

Solute speciation in supercritical aqueous alkali metal halide solutions plays an important role in various industrial and natural processes, for example, corrosion of metals, solvent extraction, crystal growth, metamorphism, and the formation of hydrothermal ore deposits. To better characterize such speciation, degrees of formation of polyatomic clusters of sodium and chlorine ions have been computed with the aid of dissociation constants generated from Monte Carlo calculations which are consistent with both supercritical conductance measurements and electrostatic theory. The calculations indicate that the solute in alkali-halide solutions is successively dominated by increasingly complex polyatomic clusters as the solute molality increases at pressures and temperatures where the dielectric constant of water is ≤ 15.

Much of what is known about solute speciation in supercritical aqueous electrolyte solutions comes from high-temperature measurements of the specific conductances of dilute (<0.1 molal) alkali metal halide solutions (*1*). These low concentration conductance data were originally interpreted by assuming that monatomic ions and diatomic neutral ion pairs are the only solute species in solution and that the activity coefficients of neutral ion pairs can be regarded as unity in dilute solutions. Although valid at molalities <0.1, these assumptions have, due to a lack of experimental data, been applied to more concentrated solutions (*2*). However, recent advances in high-temperature solution chemistry indicate that this practice is inconsistent with reality and that serious error may result from failure to take into account formation of polyatomic clusters in concentrated supercritical electrolyte solutions.

The dielectric constant of the solvent controls to a large extent the degree to which solute species associate in aqueous electrolyte solutions (*3*). The dielectric constant (ε) of H_2O at 25°C and 1 bar is

---

E. H. Oelkers, Laboratoire de Géochimie, Université Paul Sabatier, 38 rue des Trente-six Ponts, 31400 Toulouse, France.
H. C. Helgeson, Department of Geology and Geophysics, University of California, Berkeley, CA 94720–4767.

*To whom correspondence should be addressed.

~78, but it decreases to ~15 or less at low pressures and high temperatures in the supercritical region (4). The latter value is similar in magnitude to those of organic solvents at 25°C and 1 bar. The stoichiometries of polyatomic ion clusters in solutions of single electrolytes in a number of solvents with low dielectric constants ($\epsilon \leq 15$) have been investigated experimentally at temperatures $\leq 25°C$ at 1 bar (5). These studies have shown that association of the solute species in such solvents increases with increasing solute concentration from single ions and diatomic neutral ion pairs in dilute solutions to triple, quadruple, quintuple, and successively larger clusters at higher concentrations. Hence in supercritical, single electrolyte solutions at temperatures and pressures where the dielectric constant of H_2O is of the order of 15 or less, these same higher order polyatomic clusters would be expected to successively predominate with increasing concentration. This hypothesis is supported by revised interpretation of conductance measurements (6), electrostatic theory (7), and dissociation constants generated from Monte Carlo calculations (8, 9), all of which indicate that the solute in electrolyte solutions consists predominately of monatomic ions and diatomic neutral ion pairs only in the dilute concentration range at supercritical pressures and temperatures when ϵ of H_2O is ≤ 15. Thermodynamic calculations indicate that under these conditions the degree of diatomic neutral ion pair formation maximizes with increasing concentration at ~0.1 to 0.5 m (depending on the precise pressure and temperature), where m is the molality, and becomes small at higher concentrations, where neutral and singly charged polyatomic clusters (for example, triple, quadruple, quintuple, and sextuple clusters) predominate. The purpose of this report is to present the results of these calculations for a representative electrolyte (NaCl) at solute concentrations $\leq 1\ m$ at supercritical pressures and temperatures, and to explore the implications of sequential association to form higher order clusters with increasing solute concentration above 1 m.

The degrees of formation (α_i) in NaCl solutions of diatomic ion pairs ($NaCl^0$) and triple (Na_2Cl^+ and $NaCl_2^-$), quadruple ($Na_2Cl_2^0$), quintuple ($Na_3Cl_2^+$ and $Na_2Cl_3^-$), and sextuple ($Na_3Cl_3^0$) clusters can be calculated from

$$\alpha_i \equiv \nu_{Na^+,i}\left(\frac{m_i}{m}\right) \qquad (1)$$

where $\nu_{Na^+,i}$ refers to the number of moles of Na^+ ions in 1 mol of the ith cluster, m denotes the total molality of NaCl in solution, and m_i stands for the molality of the subscripted cluster. The fraction of NaCl present as Na^+ in solution (α_{Na^+}) is then

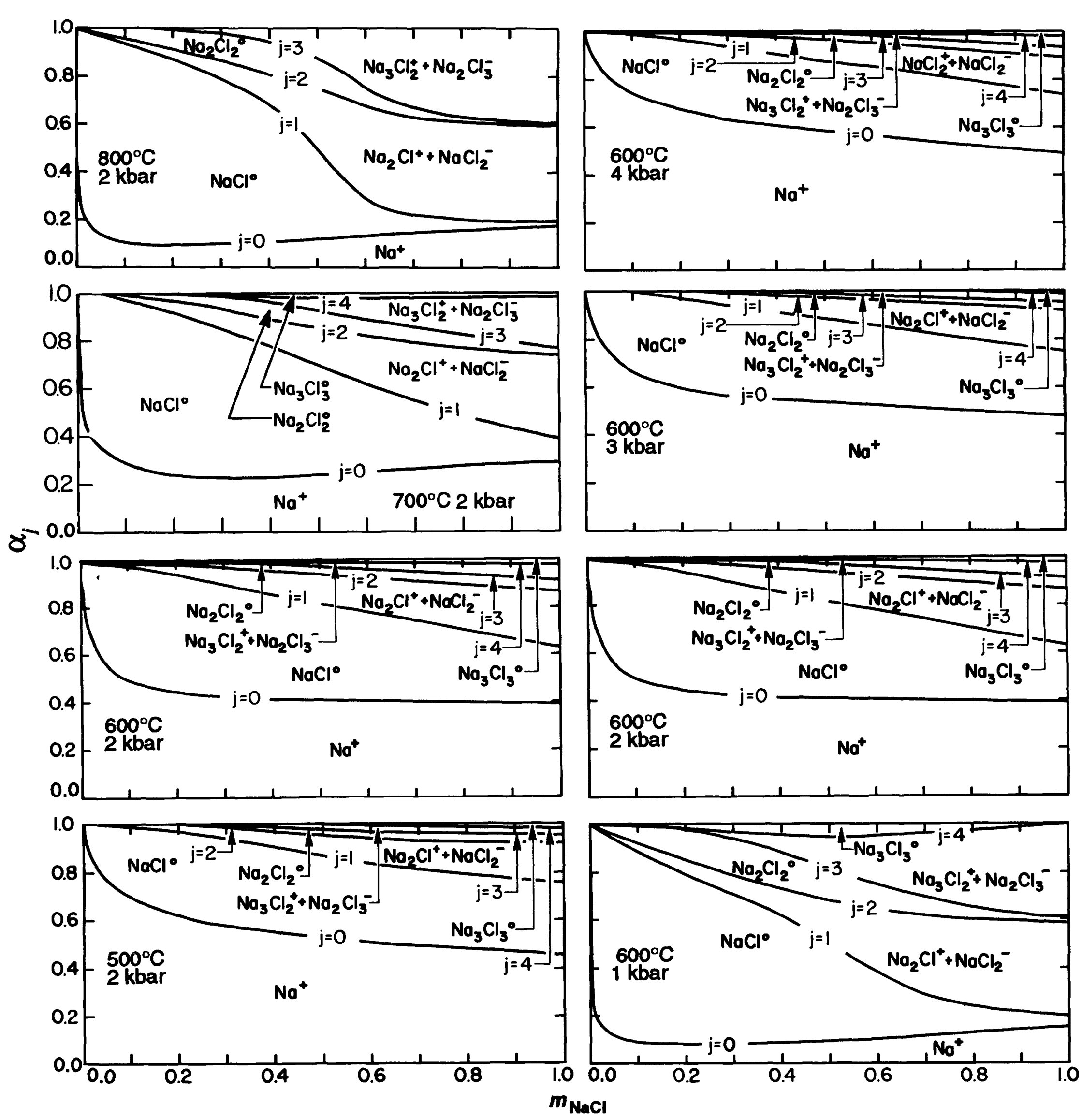

Fig. 1. Distribution diagrams indicating the degrees of formation of Na^+, $NaCl^0$, Na_2Cl^+, $NaCl_2^-$, $Na_2Cl_2^0$, $Na_3Cl_2^+$, $Na_2Cl_3^-$, and $Na_3Cl_3^0$ in NaCl solutions at supercritical pressures and temperatures (see text). The curves in these diagrams divide any vertical line drawn for a given value of m_{NaCl} into segments that are equal to the fraction of each species present in solution at the specified m_{NaCl}. Hence, α_{Na^+} in Eq. 2 and α_i for each cluster in Eqs. 1 and 3 are represented in these diagrams by the distance between the curves, which correspond to $\hat{\alpha}_j$ in Eq. 3 for j = 0,1,. . .5.

$$\alpha_{\mathrm{Na}^+} = 1 - \sum_{i=1} \alpha_i \qquad (2)$$

which is consistent with

$$\hat{\alpha}_j \equiv \alpha_{\mathrm{Na}^+} + \sum_{i=0}^{j} \alpha_i \qquad (3)$$

Distribution diagrams generated from Eqs. 1 to 3 are depicted in Figs. 1 and 2 for Na^+, NaCl^0, $\mathrm{Na_2Cl}^+$, $\mathrm{NaCl_2}^-$, $\mathrm{Na_2Cl_2}^0$, $\mathrm{Na_3Cl_2}^+$, $\mathrm{Na_2Cl_3}^-$, and $\mathrm{Na_3Cl_3}^0$ at various constant pressures and temperatures (*10–15*). The degrees of formation shown in these figures indicate that neutral ion pairs are less abundant than either single, triple, or quintuple ions in 1 *m* NaCl solutions at low pressures and high temperatures where ϵ of H_2O is ≤ 15. In contrast, triple ions account for ~6% of the solute in 0.1 *m* solutions at 600°C and 1 kbar, diminishing to <1% at 0.01 *m* NaCl. Single ions and diatomic neutral ion pairs predominate in a maximum of solution at all temperatures and pressures in 0.1 and 0.01 *m* NaCl solutions. However, triple, quadruple, quintuple, and sextuple clusters are all present in appreciable concentrations in 1 *m* NaCl solutions at 600°C, and the degrees of formation of these species increase with decreasing pressure from 4 to 1 kbar. The degrees of formation of clusters of three or more monatomic ions also increase with increasing temperature at constant pressure. The values of $\hat{\alpha}_j$ and α_i for the diatomic neutral ion pairs shown in Figs. 1 and 2 maximize with increasing solute concentration, which is also true of $\alpha_{\mathrm{Na_2Cl_2}^0}$ and $\alpha_{\mathrm{Na_3Cl_3}^0}$. Although it can be seen in these figures that the degrees of formation of the triple and quintuple ions increase monotonically and become major species with increasing NaCl concentration up to 1 *m*, they should maximize at higher solute concentrations where higher order charged clusters would be expected to be the predominant solute species. This behavior of electrolytes in solutions of low dielectric constants with increasing concentration was anticipated by Kraus (*16*).

The paucity of conductance and spectroscopic data for concentrated electrolyte solutions at supercritical temperatures and pressures, together with interpretative ambiguities, makes it difficult to compute speciation in alkali metal halide solutions at concentrations greater than 1 *m*. However, circumstantial evidence of the nature of speciation in these concentrated solutions can be inferred from other data. For example, consideration of supercritical solubility, vapor pressure, density, and phase equilibrium data for 1:1 electrolyte solutions led Valyashko (*17*) to conclude that insufficient uncoordinated H_2O dipoles were available in these solutions to solvate the solute species at concentrations in excess of 6 to 10 *m*. At these and higher concentrations, strong interionic bonding pervades the solute and significantly alter the nature of molecular interactions characteristic of the solutions at lower concentrations. The physical properties of highly concentrated electrolyte solutions at supercritical temperatures and pressures are apparently similar to those of an ionic melt containing isolated H_2O dipoles (*17*). It follows that the conductances of these concentrated solutions should be large, even though they are highly associated. This observation is consistent with the high experimental conductances reported by Hwang *et al.* (*18*) for concentrated LiCl, LiBr, and KCl solutions at 1, 2, and 3 kbar and temperatures up to 600°C, but not with their

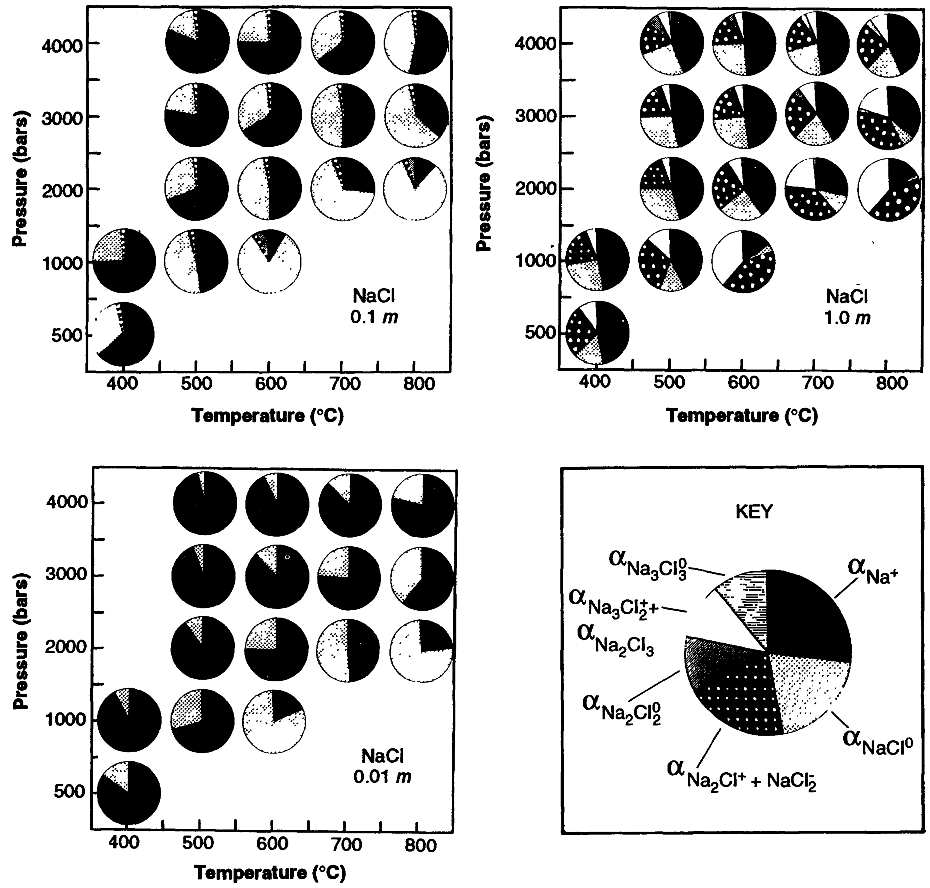

Fig. 2. Circular distribution diagrams for 0.01, 0.1, and 1.0 *m* aqueous NaCl solutions at supercritical pressures and temperatures (see text). The sectors in the diagrams represent degrees of formation of the species shown in the key.

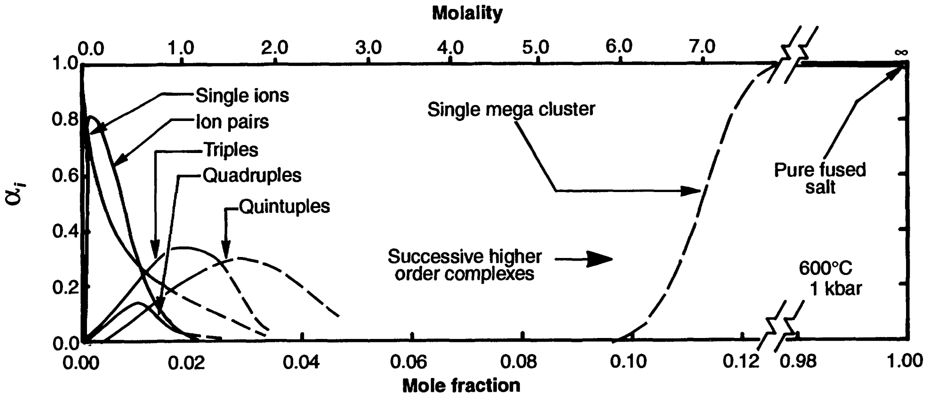

Fig. 3. Schematic depiction of likely speciation in NaCl solutions at 600°C and 1 kbar as a function of solute concentration from a dilute solution to a fused salt. The solute consists predominantly of increasingly complex polyatomic clusters with increasing concentration, which results in a single megacluster at saturation.

conclusion that the high conductances indicate complete dissociation.

The continuous change in the internal structure of electrolyte solutions with increasing concentration toward that of an ionic melt is represented by the solubility curve for halite as a function of temperature, which is continuous with the melting curve for the salt at pressures >400 bars (*19*). It thus appears that the structure of a saturated electrolyte solution at supercritical pressures and temperatures, where $\epsilon \leq 15$, may consist of a single macroscopic cluster, a megacluster, of essentially all of the solute species in solution. Such a cluster represents the culmination of the sequential formation of successively higher order clusters with increasing concentration as the solution approaches the state of a molten salt (Fig. 3).

Due to the paucity of experimental data, the calculations summarized above should be regarded as yielding provisional estimates only. Nevertheless, it appears that speciation in concentrated supercritical aqueous single-electrolyte solutions may be more complex than was generally thought to be the case. Depending on the temperature and pressure, speciation in these solutions may be dominated by successively higher order clusters at progressively higher solute concentrations. The presence of these polyatomic clusters may profoundly affect the thermodynamic properties of concentrated electrolyte solutions, as well as the solubilities of minerals in these solutions at supercritical pressures and temperatures.

REFERENCES AND NOTES

1. E. U. Franck, *Phys. Chem.* **8**, 92 (1956); G. Ritzert and E. U. Franck, *Bunsen. Phys. Chem.* **72**, 798 (1968); A. S. Quist and W. L. Marshall, *J. Phys. Chem.* **72**, 648 (1968); *ibid.*, p. 1545; L. A. Dunn and W. L. Marshall, *ibid.* **73**, 723 (1969); J. D. Frantz and W. L. Marshall, *Am. J. Sci.* **282**, 1666 (1982).
2. D. A. Sverjensky, in *Thermodynamic Modeling of Geologic Materials: Minerals, Fluids and Melts*, I. S. E. Carmichael and H. P. Eugster, Eds., vol. 17 of *Reviews in Mineralogy* (Mineralogical Society of America, Washington, DC, 1987), pp. 177–209; H. P. Eugster and L. Baumgartner, *ibid.*, pp. 367–404.
3. H. S. Harned and B. B. Owen, *The Physical Chemistry of Electrolyte Solutions* (Reinhold, New York, 1958); H. C. Helgeson and D. H. Kirkham, *Am. J. Sci.* **276**, 97 (1976); J. V. Walther and J. Schott, *Nature* **322**, 635 (1988); R. W. Gurney, *Ionic Processes in Solution* (Dover, New York, 1962); F. Franks, in *Water, A Comprehensive Treatise*, F. Franks, Ed. (Plenum, New York, 1973), vol. 2, pp. 1–54; P. V. Brady and J. V. Walther, *Geochim. Cosmochim. Acta* **54**, 1555 (1990); J.-L. Dandurand and J. Schott, *J. Phys. Chem.* **96**, 7770 (1992).
4. J. W. Johnson and D. Norton, *Am. J. Sci.* **291**, 541 (1991).
5. R. M. Fuoss and C. A. Kraus, *J. Am. Chem. Soc.* **55**, 3614 (1933); H. S. Young and C. A. Kraus, *ibid.* **73**, 4732 (1951); D. T. Copenhafer and C. A. Kraus, *ibid.*, p. 4557; M. Hojo, A. Tanio, Y. Miyauchi, Y. Imai, *Chem. Lett.* **1991**, 1827 (1991).
6. E. H. Oelkers and H. C. Helgeson, *Geochim. Cosmochim. Acta* **55**, 1235 (1991).
7. ______ *ibid.* **54**, 727 (1990).
8. K. S. Pitzer and D. R. Schreiber, *Mol. Phys.* **60**, 1067 (1987).
9. E. H. Oelkers and H. C. Helgeson, *Geochim. Cosmochim. Acta* **57**, 2673 (1993).
10. Values of $\hat{a}_j$ and α_j for supercritical NaCl solutions were calculated by minimizing the Gibbs free energy of the solution by using apparent standard partial molal Gibbs free energies of formation ($\Delta\overline{G}°$) of the solute species computed from logarithms of the overall dissociation constants (log β) of diatomic neutral ion pairs and polyatomic clusters (*9*) and values of $\Delta\overline{G}°$ for monatomic ions were calculated from the revised HKF equations of state (*11*). The standard state used in the calculations consisted of unit activity of the solute in a hypothetical 1 *m* solution referenced to infinite dilution at any pressure and temperature. The values of log β for triple, quadruple, quintuple, and sextuple clusters were generated from the results of Monte Carlo calculations (*12*) for the restricted primitive model by replacing the arbitrary hard sphere diameter (δ_H) used in these calculations with temperature- and pressure-dependent values obtained by regression of the logarithms of experimental dissociation constants (*1, 9, 13*) for diatomic neutral ion pairs (log *K*) with the molal analog of Gillan's (*12*) equation 9. This procedure renders the results of the Monte Carlo calculations consistent with the conductance data from which the values of log *K* were generated (*13*). The values of log β for triple ions computed in this manner are in general agreement with those predicted from electrostatic theory. The speciation calculations were carried out assuming the degrees of formation of septuple and larger clusters to be negligible at NaCl concentrations <1 *m*. Activity coefficients for charged and neutral aqueous species computed from the Hückel (*7, 14*) and Setchénow (*6, 15*) equations, respectively, were used in the calculations to account for cluster-cluster and cluster-solvent interactions with increasing solute concentration. The activity coefficients of the charged and neutral clusters were assumed in a first approximation to be equal to those of NaCl and $NaCl^0$, respectively.
11. E. L. Shock, E. H. Oelkers, J. W. Johnson, D. A. Sverjensky, H. C. Helgeson, *J. Chem. Soc. Faraday Trans.* **88**, 803 (1992); J. W. Johnson, E. H. Oelkers, H. C. Helgeson, *Comput. Geosci.*, **18**, 899 (1992).
12. M. J. Gillan, *Mol. Phys.* **49**, 421 (1983).
13. E. H. Oelkers and H. C. Helgeson, *J. Phys. Chem.* **92**, 1631 (1988).
14. H. C. Helgeson, D. H. Kirkham, G. C. Flowers, *Am. J. Sci.* **281**, 1249 (1981).
15. M. Setchénow, *Ann. Chim. Phys.* **25**, 225 (1892).
16. C. A. Kraus, *J. Phys. Chem.* **58**, 673 (1954); *ibid.* **60**, 129 (1956).
17. V. M. Valyashko, *Bunsen Phys. Chem.* **81**, 388 (1977).
18. J. U. Hwang, H. D. Ludemann, D. Hartmann, *High Pressures High Temperatures* **2**, 651 (1970).
19. T. S. Bowers and H. C. Helgeson, *Geochim. Cosmochim. Acta* **47**, 1247 (1983).
20. This research was supported by the National Science Foundation (NSF grant EAR-8606052), the Department of Energy (DOE grant DE-FG03-85ER-13419), and the Committee on Research at the University of California. We thank B. Ransom, W. Murphy, J. Johnson, D. Sverjensky, V. Pokrovskii, E. Shock, J. Schott, C. Monnin, and J. Amend for discussions and assistance; J. Bossart for word processing; R. Arington, K. Hwang, and Christine Owens for drafting the figures; J. Hampel and P. Gennaro for photographic assistance; and the reviewers for helpful suggestions and constructive criticism.

12 March 1993; accepted 16 June 1993

Protein Catalysis of the Retinal Subpicosecond Photoisomerization in the Primary Process of Bacteriorhodopsin Photosynthesis

Li Song, M. A. El-Sayed,* J. K. Lanyi

The rate of retinal photoisomerization in wild-type bacteriorhodopsin (wt bR) is compared with that in a number of mutants in which a positively charged (Arg^{82}), a negatively charged (Asp^{85} or Asp^{212}), or neutral hydrogen bonding (Asp^{115} or Tyr^{185}) amino acid residue known to be functionally important within the retinal cavity is replaced by a neutral, non–hydrogen bonding one. Only the replacements of the charged residues reduced the photoisomerization rate of the 13-*cis* and *all-trans* isomers present in these mutants by factors of ~1/4 and ~1/20, respectively. Retinal photo- and thermal isomerization catalysis and selectivity in wt bR by charged residues is discussed in terms of the known protein structure, the valence-bond wave functions of the ground and excited state of the retinal, and the electrostatic stabilization interactions within the retinal cavity.

Bacteriorhodopsin (bR), the other natural photosynthetic system besides chlorophyll, is a light-transducing protein present in the purple membrane of *Halobacterium halobium*. Since its discovery by Oesterhelt and Stoeckenius (*1*) in 1971 and the demonstration of its role in adenosine triphosphate (ATP) synthesis by Racker and Stoeckenius (*2*), numerous studies have been carried out to unravel its structure and the mechanism of its function (*3*). Not only is bR an important natural solar energy converter, but it is also becoming a potentially important biomaterial for photonic applications (*4, 5*) with uses in holographic recording, as ultrafast diodes, in neural networks, associative memory, and it might possibly be used as the "eyes of robots" (*5*).

L. Song and M. A. El-Sayed, Department of Chemistry and Biochemistry, University of California, Los Angeles, Los Angeles, CA 90024–1569.
J. K. Lanyi, Department of Physiology and Biophysics, University of California, Irvine, Irvine, CA 92717.

*To whom correspondence should be addressed.